Appl. Phys. B 61, 17–26 (1995)

Applied Physics B Lasers and Optics

Origin of the resonant optical Kerr nonlinearity in Cd(S, Se)-doped glasses and related topics

M. Ghanassi, L. Piveteau, L. Saviot, M.C. Schanne-Klein, D. Ricard, C. Flytzanis

Laboratoire d'Optique Quantique du C.N.R.S., Ecole Polytechnique, F-91128 Palaiseau Cedex, France
(Fax: + 33-1/6933-3017)

Received: 30 November 1994/Accepted: 6 February 1995

Abstract. After having reported preliminary results related to saturation, we first theoretically consider the various mechanisms contributing to the resonant optical Kerr effect in Cd(S, Se)-doped glasses. We obtain the expression for the expected effective susceptibility in different possible cases. This nonlinearity is studied experimentally using optical-phase conjugation in the low-intensity regime. We show that, by time resolving the nonlinear response of such glasses having experienced various degrees of photodarkening, we can clearly assess the origin of the resonant optical Kerr effect in these materials. Usually, a combination of a fast free-carrier contribution due to particles without traps and of a slow trapped-carrier one due to particles with traps is observed. For the free-carrier contribution, induced absorption is observed to be almost as important as absorption saturation. We also report frequency-dependent measurements and discuss the change in absorption spectrum and the increase of the nonradiative decay rate that accompany darkening.

PACS: 42.65; 42.70

The linear and nonlinear optical properties of semiconductor-doped glasses (SDGs) have been extensively studied in the last ten years, especially because of their potential use as nonlinear media in all-optical data processing. The most extensively studied semiconductors in this respect have been CuCl, CuBr, CdS and CdSe which correspond to different confinement regimes. Here we will concentrate on the strong confinement regime [1, 2] when the particle radius R is smaller than the exciton Bohr radius a_B and consider only CdS_xSe_{1-x} alloys with a not too large value of x. We will also concentrate on the optical Kerr effect in the one-photon resonant regime.

Most of the linear and nonlinear optical properties of these materials are now reasonably well understood. The dynamics of free-carrier recombination with the role of photodarkening and of Auger processes are well understood [3]. The line broadening mechanisms have been studied [4–6]. Estimations of the Kerr susceptibility $\chi^{(3)}$ have been made assuming that a single mechanism is operative [7]. The consequences of valence band degeneracy have been clearly established [8]. Regarding this last point, because of broadening, the samples which are used in the present work hardly show, even when taking the second derivative of the absorption spectrum, the substructure due to the $1S_{3/2}$ and $2S_{3/2}$ hole levels. We will then neglect the weak $2S_{3/2}$–$1S_e$ transition and discuss the situation in terms of a single transition, the $1S_{3/2} - 1S_e$ one.

A few points however remain unclear. The first one which is the main object of this work concerns the origin of the nonlinear response and in particular the relative magnitude of the free-carrier contribution and of the trapped carrier one. In the resonant regime, i.e. in the vicinity of the $1S_{3/2}$–$1S_e$ transition, we know that carriers are created. If the carriers remain free inside the nanocrystal, we may then expect a nonlinear response due to the saturation of the ground state to one-pair excited state transition [9] and to induced absorption corresponding to interband transitions between the one-pair and a two-pair excited state or to intraband transitions. This is what we denote the free-carrier contribution. We also know that carriers may be trapped in long-lived states and that these trapped carriers may also modify the optical properties of the semiconductor nanoparticles [10–12] either through the static electric field they create or through phase space filling. This is what we denote the trapped carrier contribution.

However, neither the range of applicability of the different mechanisms nor their relative contributions to the effective Kerr susceptibility have been clearly delineated. Intensity-dependent measurements of the $\chi^{(3)}(\omega, -\omega, \omega)$ and of the $\chi^{(3)}(\omega, -\omega, \omega)/\alpha(\omega)$ spectra, α being the absorption coefficient, carried out on $CdS_{0.4}Se_{0.6}$ doped samples using optical phase conjugation were interpreted as follows [13]: at low laser intensity, the dominant contribution is the trapped-carrier one, whereas at higher laser intensity the free-carrier

contribution becomes dominant. Here we address more quantitatively the relative contribution of these two mechanisms taking into account two aspects that have been overlooked in [13]. First, when the laser beam intensity is increased, the phase conjugate beam intensity saturates and is no longer proportional to the Kerr susceptibility squared. Secondly, frequency-dependent measurements are not the clearest way of distinguishing the two contributions as we will see below.

Another point also remains unclear. One may wonder whether there is only one class of particles contributing to both kinds of nonlinearities or two classes of particles, particles without traps which would lead to the free-carrier contribution and particles with traps which would lead to the trapped carrier contribution. Intensity-dependent luminescence measurements cannot answer this question. On the basis of time-resolved luminescence however, it was concluded [14] that the deep trap luminescence and the band edge luminescence originate from different nanocrystals. We will also address this point in the following.

This paper is organized as follows. We will present the experimental techniques and discuss preliminary experiments in Sect. 1. In Sect 2, we will discuss the various mechanisms which may contribute to the resonant Kerr susceptibility of SDGs and give the expressions of the corresponding terms in the effective Kerr susceptibility in both cases of a single class of particles and of two classes. In Sect. 3, we will show that, by time resolving the nonlinear response of samples having experienced various degrees of photodarkening, we can clearly assess the relative magnitude of the free-carrier contribution and of the trapped-carrier one and further support the hypothesis of two different classes of particles. In Sect. 4, we will report on frequency-dependent measurements and see that they do not allow to make the difference between the free-carrier contribution and the trapped-carrier one. In the light of the previous discussion, we will finally devote Sect. 5 to speculations on the consequences of photodarkening which is still also an unclear point in the physics of SDGs.

1 Experimental techniques and preliminary experiments

Most of the samples we have studied are either commercial CdS_xSe_{1-x} Schott filters such as RG 630 or experimental samples having the same chemical composition as the RG 630 filters, $x = 0.4$. For these samples whose thickness is ≈ 0.4 mm, the mean particle radius R is ≈ 4 nm. We used two different experimental techniques. Most of the measurements have been performed using an optical phase conjugation set-up with copolarized forward pump and probe beams (the pulses being time coincident) which create a population grating. This grating is probed by a cross-polarized backward pump beam and the diffracted (phase conjugate) pulse energy is measured. The three incident pulses are derived from the same laser pulse so that, when working at low intensity, the conjugate pulse energy is proportional to the cube of the laser pulse energy. In time-resolved measurements, the backward pump pulse is delayed. We also performed frequency-dependent measurements by tuning the laser wavelength and working at "zero" delay. What we call "zero" delay is the delay for which the conjugate pulse energy is maximum. We also used the nonlinear absorption technique with a single beam. In this case, we simply measure the sample transmission as a function of the incident laser pulse energy.

The laser we used is a distributed feedback dye laser (DFDL) tunable between 560 and 610 nm and delivering a 25 ps pulse. It is pumped by the second harmonic ($\lambda = 532$ nm) of a Nd : YAG picosecond pulse. Its intensity may be varied using neutral density filters or a Babinet-Soleil compensator and a polarizer. It provides the single beam needed in the case of nonlinear absorption or, when properly split, the three incident beams required by the phase conjugation set-up. Most of the measurements reported here have been performed at room temperature.

Using the nonlinear absorption technique and plotting the sample transmission as a function of the logarithm of the laser pulse energy, we typically obtain results such as the one shown in Fig. 1a. Since we are in the transient regime in which the laser pulse duration t_p is

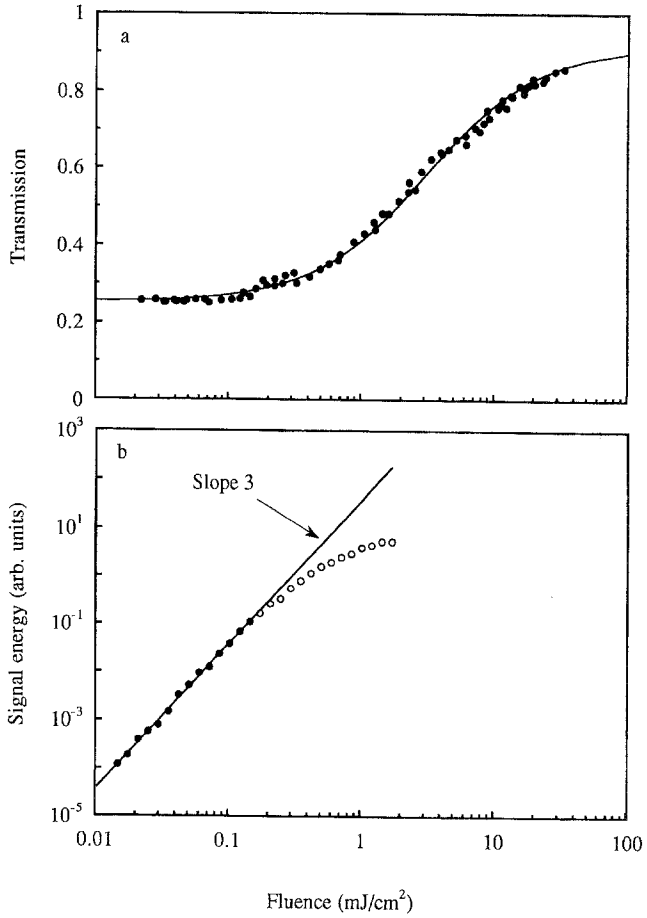

Fig. 1. **a** Transmission as a function of the logarithm of the incident fluence for an experimental Schott glass having a mean particle radius of 42 Å. The *filled circles* correspond to the data and the *solid line* to a fit as explained in the text. **b** Log-log plot of the conjugate pulse energy as a function of the total fluence of the pump beams. The *solid line* indicates the third-order power dependence observed at low laser intensity

smaller than the recombination time, the relevant quantity is the laser fluence. Whereas at low incident fluence the sample transmission assumes its low intensity value, absorption starts to saturate and transmission to increase when the laser fluence is increased. We recall that the first nonlinear optical property ever observed in SDGs was absorption saturation [15].

Experimental data such as shown in Fig. 1a are fitted assuming the transmission T to be of the form

$$T = T_\infty \exp\left(\frac{-\alpha L}{1+\phi/\phi_s}\right), \tag{1}$$

where α is the linear absorption coefficient, L the sample thickness, ϕ the incident fluence and ϕ_s the saturation fluence. T_∞ takes background or induced absorption into account [5, 16]. Equation (1) may not exactly correspond to the experimental situation since the samples are not optically thin and Auger recombination leads to an intensity-dependent effective recombination time at high fluence. But it should be accurate enough to give us the order of magnitude of the saturation fluence. We then typically get saturation fluences on the order of 1 mJ cm^{-2}.

Equation (1) also assumes homogeneous broadening. When inhomogeneous broadening dominates, the intensity dependence of transmission is different [17]. The $1S_{3/2}$–$1S_e$ transition of our samples is homogeneously broadened at room temperature [6]. At liquid N_2 temperature, inhomogeneous broadening mainly due to size dispersion usually dominates, but the use of (1) still allows us to determine ϕ_s with sufficient accuracy.

Using the phase conjugation set-up and working at a fixed wavelength and at a fixed delay for the backward pump pulse, we also varied the laser pulse energy. A typical result is shown in Fig. 1b in which a log-log plot of the conjugate pulse energy as a function of the laser pulse energy is shown. At low laser intensity, we observe a slope of 3 as expected when the third-order term dominates but, when the laser pulse energy is increased, we observe saturation of phase conjugation. Similar observations have already been reported [10] in the exponential tail of the absorption spectrum of commercial OG 530 filters. Our results show that it also applies in the case of resonant excitation. For each sample, saturation of absorption and of phase conjugation sets in at about the same value of the laser fluence (pump pulse fluence for phase conjugation).

One may wonder whether, even in the saturated regime, one could still study the material's nonlinearity by introducing a generalized $\chi^{(3)}$. Consideration of the simple case of an ensemble of two-level systems readily shows that saturation of absorption and of phase conjugation cannot be easily disentangled. We therefore come to the conclusion that only low intensity phase conjugation measurements performed in the $\chi^{(3)}$ or unsaturated regime may lead to meaningful results. In the remaining of this paper, we will then confine ourselves to phase conjugation measurements performed in such a low-intensity regime.

Nonlinear absorption measurements are however useful. They provide an independent measurement of the magnitude of the Kerr susceptibility $\chi^{(3)}$. In the resonant case, generalizing the two-level system result, we may quite generally expect $\chi^{(3)}$ to be inversely proportional to the saturation intensity. In the transient regime, we measure, using optical phase conjugation, an effective susceptibility $\chi^{(3)}_{\text{eff}}$ and, using nonlinear absorption, a saturation fluence ϕ_s. It may easily be shown that $\chi^{(3)}_{\text{eff}}$ and ϕ_s are also inversely proportional.

This is indeed what we observe. ϕ_s is smaller for experimental samples than for commercial ones in the same way as $\chi^{(3)}_{\text{eff}}$ is larger for experimental samples. ϕ_s is smaller at liquid N_2 temperature than at room temperature in the same way as $\chi^{(3)}_{\text{eff}}$ is larger at liquid N_2 temperature. This is probably due to the narrowing of the resonance upon cooling. ϕ_s is smaller for a fresh sample than for a photodarkened one in the same way as $\chi^{(3)}_{\text{eff}}$ is larger for a fresh sample. Finally, we observe that ϕ_s is not strongly frequency dependent in the vicinity of the resonance at room temperature. This is probably due to the large (homogeneous) width of this resonance.

2 Background considerations

Before presenting experimental results which allow us to determine the origin of the nonlinear response, we discuss in this section the expressions of the Kerr susceptibility we expect in different situations: the case of one class of particles and the case of two classes, one without traps, the other one with traps. We also keep in mind that, in the transient regime, we measure an effective Kerr susceptibility. As we will see, this is equivalent to using the response function approach.

2.1 The basic model

As possible mechanisms of the nonlinear response we know, as already stated in the Introduction, that we may have a free-carrier contribution and a trapped-carrier one. Our discussion will be based on Fig. 2 which shows the

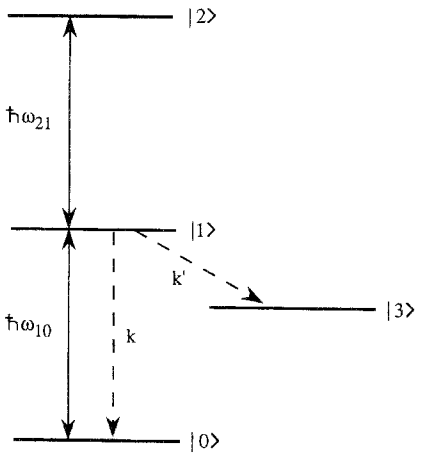

Fig. 2. Level scheme corresponding to the physical situation of a quantum dot. Level 0 is the ground state of the dot, level 1 is the $1S_{3/2}$–$1S_e$ excited state, level 2 may correspond to a two pair excited state and is further discussed in the text and level 3 describes trapped carriers. k is the direct decay rate from level 1 to level 0 and k' is the trapping rate of carriers. We consider the situation $\omega \approx \omega_{10} \approx \omega_{21}$

four relevant levels for a given particle in our basic model. Level 0 is the ground state of the nanocrystal. Level 1 corresponds to the $1S_{3/2}$–$1S_e$ excited state. From level 1, we may have induced absorption towards level 2. We will discuss the possible states corresponding to level 2 below. Level 3 corresponds to trapped carriers. The luminescence band due to trapped carrier recombination is fairly broad. For our purposes however, it is sufficient to describe trapped carriers in terms of a single level. On the time scale of our experiment (a few nanoseconds), we neglect relaxation of trapped carriers which takes place on the microsecond range.

We limit ourselves to the case where the two transition frequencies ω_{10} and ω_{21} are nearly equal and $\omega \approx \omega_{10} \approx \omega_{21}$. We first note that, for a three-level system (for example levels 0, 1 and 2) and keeping only the fully resonant terms, the expression for the hyperpolarizability γ is easily obtained [18]. In our case, with very rapid dephasing, the expression for γ or the change in polarizability $\Delta\alpha_{pol}$ is simply related to the change in population of levels 0, 1 and 3, i.e. to the creation of carriers and their subsequent trapping. For the phase conjugation set-up, with our choice of polarizations, this change in population originates from the population grating due to interference between the forward pump and probe beams.

We denote ρ_{ii} the occupation probability of level i. At thermal equilibrium $\rho_{00} = 1, \rho_{11} = \rho_{22} = \rho_{33} = 0$. For the level scheme shown in Fig. 2, the linear polarizability $\alpha_{pol}(\omega)$ of a particle at frequency $\omega \approx \omega_{10}$ is then given by

$$\alpha_{pol}(\omega) = \frac{\mu_{10}^2 T_2}{\hbar(\delta - i)}, \tag{2}$$

where μ_{10} is the transition matrix element of the dipole moment, T_2 the dephasing time and $\delta = (\omega_{10} - \omega)T_2$ is the normalized detuning. The linear absorption coefficient α is given by

$$\alpha(\omega) = \frac{\omega}{nc} 4\pi N |f(\omega)|^2 \operatorname{Im} \alpha_{pol}(\omega), \tag{3}$$

where n is the index of refraction of the glass sample, N the number density of particles and $f(\omega)$ the local field factor which relates the field inside the particle to the field in the glass matrix [19]:

$$f(\omega) = \frac{3\varepsilon_d}{\varepsilon(\omega) + 2\varepsilon_d} \tag{4}$$

$\varepsilon(\omega)$ being the dielectric constant of the semiconductor particle and ε_d that of the glass matrix.

The occupation probabilities ρ_{11}, ρ_{33} and ρ_{00} obey the equations

$$\frac{d\rho_{11}}{dt} = \frac{\sigma I(t)}{\hbar\omega} - (k + k')\rho_{11}, \tag{5a}$$

$$\frac{d\rho_{33}}{dt} = k'\rho_{11}, \tag{5b}$$

$$\frac{d\rho_{00}}{dt} = -\frac{\sigma I(t)}{\hbar\omega} + k\rho_{11} + k'\rho_{11}. \tag{5c}$$

Equations (5a) and (5b) and the first two terms of (5c) are self-explanatory with $\sigma = \alpha/N$ the absorption cross-section of a particle, $I(t) = (nc/8\pi)\, A_f(t)A_p^*(t)$ and the decay rates k and k' as indicated in Fig. 2. The lifetime T_1 of level 1 is $1/(k + k')$. The three incoming fields are defined in the glass matrix as

$$\mathbf{E}_i(r, t) = \tfrac{1}{2}\mathbf{A}_i(t)e^{i(\mathbf{k}_i \cdot \mathbf{r} - \omega t)} + c.c.,$$

with i = f, b, p standing for forward, backward and probe. We will assume for simplicity that the A_i's are real but we write $A_f A_p^*$ to keep in mind that we consider phase conjugation. The last term in (5c) is due to the following: when an electron is trapped from state $1S_e$, it empties this state and when a hole is trapped from state $1S_{3/2}$, an electron from the trap refills the $1S_{3/2}$ state so that when a pair is trapped, the system relaxes from level 1 to level 0.

The trapping time constant $1/k'$ has been observed to be very short [20, 21]. In this section however, we do not make any assumption about the magnitude of k' in order to obtain general results which will be needed later on for the discussion of special cases.

For a general laser pulse shape, (5) may be solved numerically using, for instance,

$$\rho_{11}(t) = \int_{-\infty}^{t} \frac{\sigma I(t')}{\hbar\omega} e^{-(k+k')(t-t')}\, dt'. \tag{6}$$

They may be solved analytically in the case of rectangular pulses, $I(t) = I$ when $0 < t < t_p$ and 0 otherwise. Since Gaussian pulses lead to very close results, we will use the analytical results obtained in the rectangular pulse case. Then, when $t > t_p$, for example, we have

$$\rho_{11}(t) = \frac{\sigma I}{\hbar\omega}\frac{1}{k + k'}[1 - e^{-(k+k')t_p}]e^{-(k+k')(t-t_p)}, \tag{7a}$$

$$\rho_{33}(t) = \frac{\sigma I}{\hbar\omega}\frac{k'}{k + k'} \times \left\{t_p - \frac{1}{k + k'}[1 - e^{-(k+k')t_p}]e^{-(k+k')(t-t_p)}\right\}, \tag{7b}$$

$$\rho_{00}(t) = 1 - \rho_{11}(t). \tag{7c}$$

They are also easily calculated when $0 < t < t_p$.

The change in polarizability at time t due to saturation of the $0 \rightarrow 1$ transition is given by

$$\Delta\alpha_{pol}^{abs\,sat}(t) = [\Delta\rho_{00}(t) - \rho_{11}(t)]\frac{\mu_{10}^2 T_2}{\hbar(\delta - i)} = -2\rho_{11}(t)\frac{\mu_{10}^2 T_2}{\hbar(\delta - i)}, \tag{8}$$

where $\Delta\rho_{00}$ is the change in ρ_{00} or $\rho_{00}(t) - 1$.

Since $\omega \approx \omega_{21}$, the change in polarizability at time t due to induced absorption from level 1 to level 2 is of the form

$$\Delta\alpha_{pol}^{ind\,abs}(t) = \rho_{11}(t)\frac{\mu_{21}^2 T_2'}{\hbar(\delta' - i)}, \tag{9}$$

where μ_{21} and T_2' are the corresponding transition element and dephasing time and $\delta' = (\omega_{21} - \omega)T_2'$.

At this point, we must discuss the nature of level 2 or of the $1 \rightarrow 2$ transition. We may first have interband transitions (one more pair is created) in which case level 2 corresponds to the $2(1S_{3/2} - 1S_e)$ state. We recall that level $1S_{3/2}$ is fourfold degenerate, whereas level $1S_e$ is twofold degenerate so that two electrons may be promoted from level $1S_{3/2}$ to level $1S_e$. We may also have intraband transitions in which the electron, for example, is promoted from level $1S_e$ to level nP_e. In this case, level 2 corresponds to state $1S_{3/2} - nP_e$. We may of course also have intraband transitions involving the hole inside the "valence band". Although intraband transitions do exist, they may not significantly contribute to the nonlinearity in our case. For a particle radius of ≈ 4 nm and a photon energy of 2.1 eV, the resonant nP_e level has a large n index so that the corresponding transition matrix element is very small. We do not have however to neglect intraband transitions. Since the response has the same form in both cases, we may assume (9) to describe the situation for both interband and intraband transitions. If we restrict ourselves to two-pair states, when the carrier pairs are only weakly interacting, $\mu_{21}^2 \approx 2\mu_{10}^2$ and $T_2' \approx T_2$ so that saturated absorption and induced absorption cancel each other. This cancellation effect does no longer exactly apply when the two pairs interact.

As already stated, trapped carriers modify the optical properties of the particles through phase space filling or through the static electric field they create. Wang et al. [22] already showed that, due to the poor overlap between the wave functions of free carriers and trapped carriers, phase space filling should be rather ineffective. They also put forward a model based on variational calculations to account for the consequences of Coulomb interaction between the trapped pair and the pair we want to create in the probing process. Here we will make use of a simpler model. We will assume that a trapped pair creates a static and uniform electric field of order

$$E_0 = \frac{e}{\varepsilon_0 R^2},$$

where ε_0 is the low-frequency dielectric constant of the semiconductor. This static electric field modifies the polarizability by the amount $\gamma(0, 0, \omega)E_0^2$ where $\gamma(0, 0, \omega)$ is the static Kerr polarizability. Thus, the average change in polarizability due to trapped carriers is $\Delta\alpha_{pol}^{tr}$ given by

$$\Delta\alpha_{pol}^{tr}(t) = \rho_{33}(t)\gamma(0, 0, \omega)E_0^2. \tag{10}$$

The total change in polarizability of a particle is then

$$\Delta\alpha_{pol}(t) = \Delta\alpha_{pol}^{abs\,sat}(t) + \Delta\alpha_{pol}^{ind\,abs}(t) + \Delta\alpha_{pol}^{tr}(t) \tag{11}$$

and, assuming all particles to be identical, the nonlinear source polarization for the conjugate beam is

$$P^{NL}(t) = N[f(\omega)]^2 \Delta\alpha_{pol}(t) A_p(t - \tau) \tag{12}$$

since the backward pump pulse is delayed by the amount τ. We notice that (12) is nothing but the response function approach.

Since we assume $\omega \approx \omega_{10} \approx \omega_{21}$, we have $\delta \approx \delta' \approx 0$, so that we may set with a good accuracy:

$$N[f(\omega)]^2 \frac{\sigma I}{\hbar\omega} \frac{1}{k + k'} \frac{\mu_{10}^2 T_2}{\hbar(\delta - i)} \approx ia A_f A_p^* \tag{13}$$

and

$$N[f(\omega)]^2 \frac{\sigma I}{\hbar\omega} \frac{1}{k + k'} \frac{\mu_{21}^2 T_2'}{\hbar(\delta' - i)} \approx ib A_f A_p^* \tag{14}$$

with a and b real and positive. Similarly, it is fair to assume

$$N[f(\omega)]^2 \frac{\sigma I}{\hbar\omega} t_p \gamma(0, 0, \omega) E_0^2 \approx -icA_f A_p^* \tag{15}$$

with c real and positive since electroabsorption measurements [23] show a resonant decrease in absorption in the vicinity of the $1S_{3/2}$–$1S_e$ transition.

We may then write, for $t > t_p$,

$$p^{NL}(t) = -i[S + Fe^{-(t - t_p)/T_1}] A_f A_p^* A_b(t - \tau) \tag{16}$$

with

$$S = \frac{k'}{k + k'} c \tag{17}$$

and

$$F = (1 - e^{-t_p/T_1}) \left(2a - b - \frac{k'}{k + k'} \frac{T_1}{t_p} c \right). \tag{18}$$

Neglecting the linear absorption losses which may be taken into account *a posteriori* and assuming low reflectivity, the amplitude of the conjugate wave at time t is then obtained:

$$A_c(t) = i \frac{2\pi\omega}{nc} P^{NL}(t) L. \tag{19}$$

The intensity of the conjugate beam is then $I_c(t) = (nc/8\pi)[A_c(t)]^2$ and the quantity which is measured is the fluence $\phi_c(\tau)$ of the conjugate pulse $\phi_c(\tau) = \int_{-\infty}^{+\infty} I_c(t)\, dt$. When $\tau > t_p$, this fluence is easily calculated:

$$\phi_c(\tau) = K \left\{ S^2 t_p + 2SFT_1 e^{-(\tau - t_p)/T_1} (1 - e^{-t_p/T_1}) + \frac{F^2 T_1}{2} e^{-2(\tau - t_p)/T_1} (1 - e^{-2t_p/T_1}) \right\} \tag{20}$$

with $K = (\pi\omega^2/2nc)[A_f A_p^* A_b]^2 L^2$. It is a steadily decreasing function of the backward pump pulse delay τ. The "zero" delay τ_0 is then within the interval $[0; t_p]$. When $t_p \ll T_1$ as will often be the case experimentally, then $\tau_0 \approx t_p$.

We notice that, within our approximations, $-i(2a - b)$ is the true (steady-state) susceptibility due to free carriers which we denote $\chi_{free}^{(3)}$. When $k' = 0$ (no traps), $-iF$ is then simply the effective susceptibility due to free carriers and obtained by multiplying $\chi_{free}^{(3)}$ by the factor $(1 - \exp(-t_p/T_1))$ describing the progressive filling of level 1. This factor is close to t_p/T_1 when $t_p \ll T_1$. In the same way, $-ic$ is the effective susceptibility associated with trapped carriers. The presence of t_p in the expression giving c is due to the strongly transient character of this response.

We also notice that these susceptibilities involve the four $f(\omega)$ factors as they should [19]. It has been shown in [19] that, close to the $1S_{3/2}$–$1S_e$ transition, the optical

properties of SDGs behave as if $\varepsilon(\omega)$ were approximately constant and equal to ε_∞ where ε_∞ is the high-frequency dielectric constant of the semiconductor. $f(\omega)$ is then real, frequency-independent and slightly smaller than 1.

2.2 *Two classes of particles*

The model we discussed in the previous section corresponds to the case where we have only one class of particles, all having the same properties. We now consider the case where we have two different classes of particles: one without traps denoted w/o and one with traps denoted w. The respective number densities are $N_{w/o}$ and N_w with $N_{w/o} + N_w = N$.

For the w/o particles, (7) hold with $k' = 0$ (no traps). For example, $\rho_{33} = 0$. In (13) and (14), N must be replaced by $N_{w/o}$ and k' set equal to zero. The lifetime T_1 of level 1 is now $1/k$. Equations (17) and (18) lead to $S_{w/o} = 0$ and $F_{w/o} = (1 - e^{-t_p/T_1})(2a_{w/o} - b_{w/o})$ where

$$2a_{w/o} - b_{w/o} = N_{w/o}[f(\omega)]^2 |f(\omega)|^2 \frac{\mu_{10}^2 T_2 T_1}{\hbar^2} \times \left[\frac{\mu_{10}^2 T_2}{\hbar} - \frac{1}{2}\frac{\mu_{21}^2 T_2'}{\hbar}\right]. \quad (21)$$

For the w particles, we set k' to infinity in (7) assuming trapping to be very fast. Then $\rho_{11} = 0, \rho_{00} = 1$ and $\rho_{33} = \frac{\sigma 1 t_p}{\hbar\omega}$. Equations (13) and (14) give $a_w = b_w = 0$. In (15), N must be replaced by N_w. (17) and (18) lead to $S_w = c_w$ and $F_w = 0$ with $c_w = N_w c/N$.

The expression for the total $P^{NL}(t)$ thus still has the form (16) but with

$$S = c_w \quad (22)$$

and

$$F = (1 - e^{-t_p/T_1})(2a_{w/o} - b_{w/o}). \quad (23)$$

With these new expressions for S and F, (19) and (20) are still valid and we will make use of (20) to discuss the experimental results.

2.3 *Numerical estimates*

We now give numerical estimates for the different contributions to the effective susceptibility. We start with the trapped-carrier contribution which we estimate from the linear properties and the electroabsorption measurements. With the numerical values $\alpha = 100$ cm^{-1}, $t_p = 25$ ps, $\lambda = 580$ nm, $R = 4$ nm, $\chi^{(3)}(0, 0, \omega) = 10^{-12}$ esu [23] and assuming a volume fraction of $\approx 3 \times 10^{-3}$, we get for c a number of order 10^{-10} esu.

The free-carrier contribution may be estimated from the linear properties also assuming a volume fraction of $\approx 3 \times 10^{-3}$. For the contribution due to saturation of the $0 \rightarrow 1$ transition, we then get for $2at_p/T_1$ a number of order 10^{-8} esu [19], 100 times larger than c. But, as already stated, the induced absorption mechanisms partly cancel this contribution. We recall that, when the pairs are weakly interacting, then $b \approx 2a$.

3 Time-resolved phase conjugation

We now present results obtained by time resolving the nonlinear response of samples having experienced various degrees of photodarkening. The consequences of photodarkening [24–26] are now well known. The slow component of luminescence due to trapped-carrier recombination is drastically reduced as if trapping centres were no longer existent or efficient, the nonlinear response becomes faster, the nonradiative decay rate of free carriers increases [3] and the "zero" delay effective susceptibility decreases. The absorption spectrum is not significantly altered however. We took fresh samples and deliberately darkened them by exposing them to a laser beam at $\lambda = 532$ nm for 1–2 h. The darkening beam diameter was 2.5 mm with a Gaussian profile, the pulse energy ≈ 0.6 mJ and the repetition rate 1 pulse per second. The laser beam diameter in the phase conjugation set-up was smaller (≈ 0.7 mm) so that we could probe spots on the sample having received various darkening doses. Measuring the effective susceptibility at "zero" delay, as a function of position, we got results such as the ones shown as filled circles in Fig. 3. We recall that "zero" delay is $\tau_0 \approx t_p$.

It clearly shows how photodarkening reduces the magnitude of the "zero" delay effective susceptibility. For the samples we studied, the ratio between its value for a nondarkened area and for the most darkened one may reach the value 5–6 for a commercial glass. It is typically equal to 3 for an experimental one. We recall that for these samples, commercial ones have more trapping centres than experimental ones [27]. We also observe that the decrease of the "zero" delay effective susceptibility can be fitted by a Gaussian profile reproducing the 532 nm laser profile. The minimum value of this effective susceptibility does not decrease to zero. When the darkening dose is increased, we observe a saturation of darkening, the bottom of the effective susceptibility profile becoming flat.

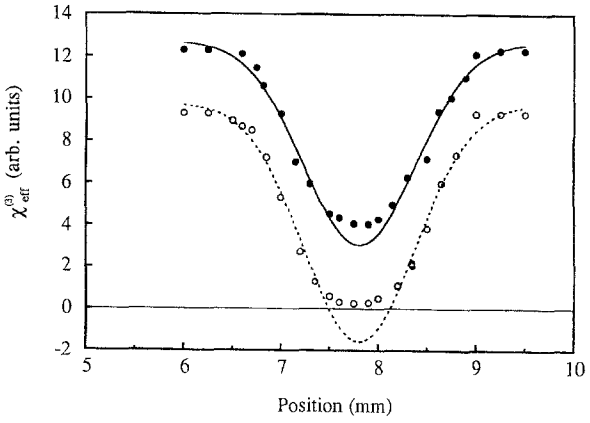

Fig. 3. The effective Kerr susceptibility plotted as a function of position for an experimental sample which has been photodarkened with a laser beam having a Gaussian profile and a diameter of 2.5 mm. The *filled circles* (data) and the *solid line* (fit) correspond to the "zero" delay case. The *open circles* (data) and the *dotted line* (fit) correspond to a delay of 1.4 ns for the backward pump pulse. In this last case, the fitting curve goes below the zero line because of saturation of photodarkening

We then choose a given position of the sample and time-resolve the nonlinear response by delaying the backward pump pulse. Two typical results are showing Fig. 4: Fig. 4a corresponding to a less darkened area and Fig. 4b to a more darkened one. In these measurements, a non-darkened spot of the sample is used as a nonlinear reference. We clearly see that the nonlinear response is made of two components, a fast component decaying exponentially with a time constant varying between ~ 1.4 ns and ~ 30 ps depending on the degree of photodarkening and a slow component whose decay constant is at least tens of nanoseconds. This is in agreement with previous observations [28]. We notice that our set-up is not well suited to measure long decay times since the DFDL beam is not perfectly collimated. It is however quite reliable when the decay time is smaller than 1 ns.

We fit our experimental data using expression (20). We determine the three fitting parameters, S, F and T_1. Notice that the sum $(S+F)$ is close to the value of the modulus of the effective susceptibility at $\tau = t_p$ delay, thus reducing the number of independent parameters to two. The $\tau = t_p$ delay is obtained as the "zero" delay when T_1 is large (fresh sample). The larger the darkening dose is, the smaller the time constant of the fast component and the smaller the relative magnitude S/F of the slow and fast components. One can get to the point where there is only a fast component. This is in agreement with the measurements reported as open circles in Fig. 3. There, the effective susceptibility was measured as a function of position for a delay $\tau = 1.4$ ns. For such a delay, the fast component has disappeared and we observe only the slow component which vanishes for the most darkened positions.

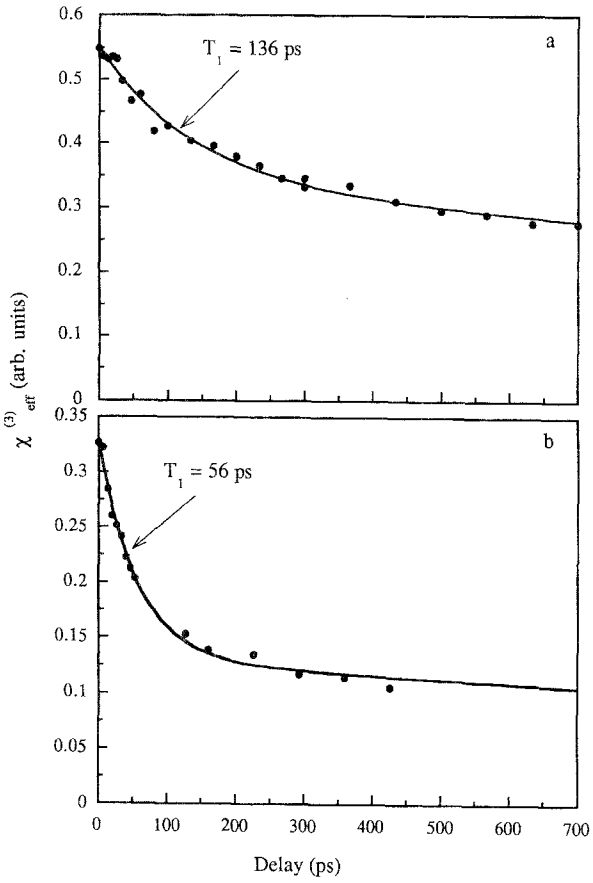

Fig. 4a,b. The effective Kerr susceptibility, proportional to the square root of the conjugate pulse energy, plotted as a function of the backward pump pulse delay for (**a**) a less darkened area and (**b**) a more darkened one. The *solid line* is a fit using (20) of the text

When working with a fresh commercial sample in the exponential tail of the absorption spectrum such as is the case for the Schott OG 530 filter at $\lambda = 532$ nm, there is usually only a slow component. Such a behaviour may explain why the $\chi^{(3)}$ profile reported in [26] goes to zero at the most darkened point. But in our case, near the $1S_{3/2}$–$1S_e$ transition, even for fresh samples, the nonlinear response is the sum of a fast and a slow component. For fresh samples, the slow component is dominant. For darkened ones, the fast component dominates.

On the basis of the response times, it seems natural to assign the slow component to trapped carriers and the fast component to free carriers as already proposed [28]. We now reconsider this in the light of the discussion we give in Sect. 2. The effective susceptibility for the slow component is proportional to the S term of (16). In both cases, one class of particles (see (17)), or two classes of particles (see (22)), S is related to trapped carriers. On the other hand, in the first case (see (18)), the magnitude of the fast component F involves both free and trapped carriers, whereas in the second case (23), it involves only free carriers in w/o particles. Now, as already stated, the trapping time $1/k'$ has been observed to be very short [20, 21]. In the first case, $T_1 = 1/(k+k')$ should be at least as short. Since the values we measure for T_1 vary from 1.4 ns to 30 ps, this rules out the one-class hypothesis. Based on the values of the time constant T_1, we then conclude that we have two classes of particles: particles without traps leading to the fast and free-carrier contribution with $T_1 = 1/k$ and particles with traps leading to the slow or trapped-carrier contribution.

The assignment of the fast component to free carriers is further supported by the following observation. If we assume only one class of particles, then the magnitude of the fast component F is given by (18), (13), (14) and (15) and involves a, b and $k'c/(k+k')$. Based on the observations that darkening does not significantly change the absorption spectrum, we may admit that μ_{10}, δ, T_2 and also presumably μ_{21}, δ' and T_2' are not modified by photodarkening. But darkening decreases the magnitude of T_1, i.e. increases the value of $k+k'$ and at the same time decreases the value of k' (traps have been deactivated). We then expect the quantity $Q = (1/(1-e^{-t_p/T_1}))\,F/T_1$ to change upon darkening. If, on the other hand, we assume two classes of particles, then F is given by (23) and (21) and involves only a and b so that, in this case, the quantity Q is expected to be independent of the degree of darkening. We have plotted in Fig. 5 this quantity Q as a function of T_1 which is here a measure of the degree of darkening. Within the experimental uncertainty, it is observed to be constant. This supports our interpretation: there are two classes of particles, the fast component is due to free carriers in w/o particles, the slow component is due to trapped carriers in w particles.

Darkening decreases the magnitude of T_1, i.e. increases the value of k for w/o particles. It also causes the disappearance of the slow component proportionately to

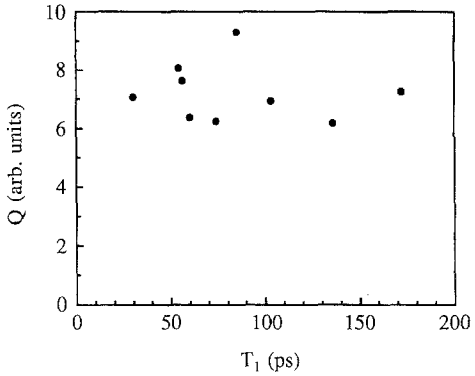

Fig. 5. Plot of $Q = (1/(1 - e^{-t_w/T_1})) F/T_1$ as a function of T_1 which is here a measure of the degree of photodarkening. See text for more details

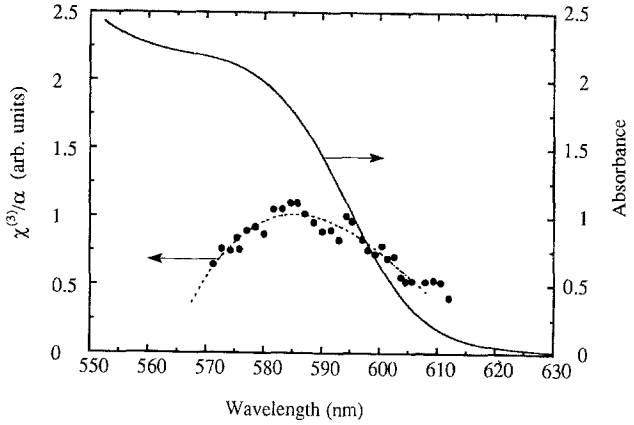

Fig. 6. Absorption $\alpha(\omega)$ spectrum and $\chi^{(3)}/\alpha$ spectrum for a fresh experimental sample with a mean particle radius of ≈ 32 Å. $\chi^{(3)}$ is the "zero" delay effective susceptibility. From the second derivative of the $\alpha(\omega)$ spectrum, we know that the $1S_{3/2}$–$1S_e$ transition occurs around $\lambda = 585$ nm. The *dotted line* is only a guide to the eye

the irradiation dose. This can be understood in the following way. Each time a w particle is "darkened" its traps are deactivated so that k' becomes zero and radiationless relaxation from level 1 to level 0 in this w particle becomes very fast so that it does not contribute any more to the nonlinear response. We will come back to the consequences of darkening in Sect. 5.

Correcting for absorption losses and using CS_2 as a nonlinear reference, we can get an estimate for the numerical values of S and F. The magnitude of the effective susceptibility S for the trapped-carrier contribution is on the order of 10^{-10} esu in agreement with the numerical estimate given at the end of Sect. 2 assuming the effect to be mediated by the static electric field created by trapped carriers. This assumes that the number densities $N_{w/o}$ and N_w are of the order of N. This is in agreement with the observation that the relative magnitude of the two luminescence bands changes from sample to sample [27]. For commercial samples, N_w is probably larger than $N_{w/o}$ but for experimental samples, they probably have the same order of magnitude. The magnitude of the fast or free-carrier contribution F is also of the order of 10^{-10} esu or less, i.e. $2a - b$ is about 100 times smaller than what we would expect by taking only saturation of the $0 \rightarrow 1$ transition into account as discussed in Sect. 2 and neglecting induced absorption. Induced absorption has been observed in the nondegenerate case [5]. Our results indicate that, in the degenerate case, it leads to an important cancellation effect.

This shows that, even when considering only the free carriers, quantum dots do not behave as simple two-level systems. We indeed know that, in the weak confinement regime, the excitonic nonlinearity vanishes in the limit of weak interaction between the excitons. The strong cancellation effect we observe may be compared with such a behaviour although we are here in the strong confinement regime. Experiments are in progress in order to understand whether such a behaviour corresponds to a general tendency.

4 Frequency-dependent phase conjugation

Working at "zero" delay, we also measured the $\chi^{(3)}/\alpha$ spectrum of our samples. $\chi^{(3)}$ is here the effective susceptibility proportional to $(S + F)$. A typical result is shown in Fig. 6. In the exponential tail of the absorption spectrum, the ratio $\chi^{(3)}/\alpha$ is observed to be frequency independent in agreement with previous observations [24] although there is no clear explanation for this fact. We take advantage of it however and use as a nonlinear reference commercial filters such as RG 610 in the exponential tail of their absorption spectrum. So doing, we are in the transient regime for both sample and reference and avoid problems due to fluctuations or drift in the laser pulse duration.

We observe in Fig. 6 a resonance in the vicinity of the $1S_{3/2}$–$1S_e$ transition. This is in agreement with previous observations [29]: notice that, in Fig. 2 of [29], the logarithm of $\chi^{(3)}$ is plotted whereas in Fig. 6 a linear plot is shown. We observe that this resonance is more apparent for experimental samples for which the transition is narrower. It is also sharper at liquid nitrogen temperature than at room temperature. We recall that, at room temperature, the broadening is mainly homogeneous or intrinsic and that the width of the $1S_{3/2}$–$1S_e$ feature in the absorption spectrum decreases when the temperature is reduced [6].

In the vicinity of the resonance, the $\chi^{(3)}/\alpha$ spectrum is about the same for a fresh and for a darkened sample when the dominant nonlinear mechanism has changed as discussed above. This supports our earlier statement that a study of this $\chi^{(3)}/\alpha$ spectrum is not the best way of assessing the origin of the nonlinearity. This is easily understandable on the basis of the discussion given in Sect. 2. For the free-carrier contribution, as is clear from (8) and (9), $\chi^{(3)}/\alpha$ should exhibit a resonance in the vicinity of the $1S_{3/2}$–$1S_e$ transition, at least when homogeneous broadening dominates. But, in the case of the trapped-carrier contribution, although c_w is proportional to the number of trapped carriers and therefore to the absorption coefficient α, assuming, for example, the nonlinearity to be given by (10), c_w is also proportional to the static Kerr polarizability $\gamma(0, 0, \omega)$ and the ratio S/α is also expected to show a resonance in the vicinity of the same transition [23].

5 Speculations on photodarkening

In this section, we tentatively discuss the photodarkening phenomenon. Specifically, we try to understand the mechanism through which darkening modifies the linear properties and dynamics of SDGs.

We first consider the permanent consequences, which are usually small, of photodarkening on the linear absorption spectrum of SDGs. Using samples grown from the same melt as the Schott RG 715 filters for which darkening is more important, carefully measuring the absorption spectrum before and after darkening and subtracting, we obtained the differential absorption spectrum shown in Fig. 7. We observe oscillations in the vicinity of the $1S_{3/2}$–$1S_e$ transition in agreement with a recent report [30]. This differential absorption spectrum was attributed to the static electric field due to carriers trapped in surface states or in the glass matrix as previously suggested [31].

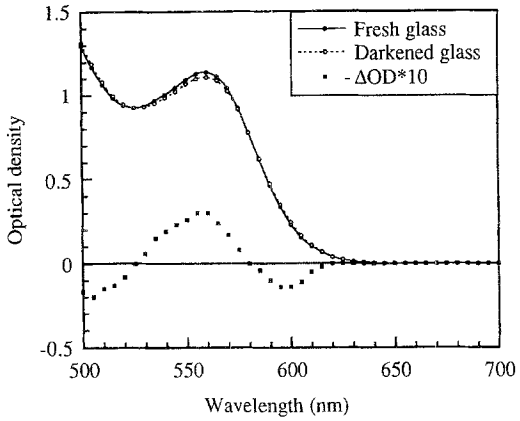

Fig. 7. Absorbance spectra of an experimental sample grown from the same melt as RG715 filters before (*solid line*) and after (*dotted line*) darkening. The *squares* indicate, on a magnified scale, the difference between the two

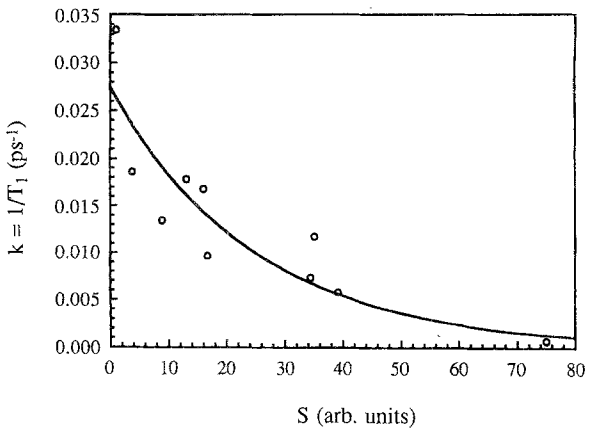

Fig. 8. Plot of the decay rate $k = 1/T_1$ of the fast component vs the magnitude S of the slow component of the effective susceptibility for spots of a commercial RG 630 sample having experienced various degrees of darkening. The *open circles* are the experimental data points – the rightmost point corresponds to the fresh sample – and the *solid line* is an exponential fit

The change in absorption coefficient we observe is small but sizable. For an absorbance of 1.10 in the vicinity of the $1S_{3/2}$–$1S_e$ peak, the maximum change in absorbance is 0.03. Assuming the same value of the dc Kerr susceptibility for RG 715 samples as for RG 610 ones [23], this corresponds to a mean electric field of about 5×10^5 V cm^{-1}. Such an electric field is large indicating that the carriers are more probably trapped at the particle surface or very close.

Coming back to our RG 630 samples, we already pointed out that darkening reduces the magnitude of the time constant T_1 and of the slow component S of the effective susceptibility. It is also interesting to look at the correlation between these two effects of darkening. We may speculate that S is proportional to the number of w particles with still active trapping centres and that "darkened" w particles enhance nonradiative recombination in w/o particles via the static electric field created by carriers trapped in the glass matrix. Figure 8 shows our experimental results with a plot of $1/T_1$ vs S together with a fit of the form

$$k = \frac{1}{T_1} \propto e^{-\kappa S}.$$

The correlation coefficient is only 88% and other functional forms cannot be ruled out. S and T_1 are obtained by deconvoluting data such as shown in Fig. 4 in terms of a fast and a slow component. This leads to significant uncertainty and is the reason for the scatter of data points in Fig. 8. In order to be more conclusive, further experiments are needed. It would, for example, be interesting to study the dependence of T_1 as a function of an applied dc field.

6 Conclusion

In summary, we have first noticed that, in order to measure quantitatively the Kerr susceptibility, saturation of phase conjugation must be avoided. Absorption saturation measurements are useful though in that they give indications on the nonlinear susceptibility. We then considered theoretically the various mechanisms leading to the nonlinear response. The free-carrier contribution which involves both absorption saturation and induced absorption is due to population changes. An expression has been derived for the trapped-carrier contribution when it is mediated by a static electric field. We also considered the form of the effective susceptibility in the two cases of a single class of particles and of two different classes, particles without traps and particles with traps.

Experimentally, using optical phase conjugation in the low-intensity regime, we observed that, by time resolving the nonlinear response of semiconductor-doped glasses having experienced various degrees of photodarkening, we are able to assess more clearly the origin of the resonant optical Kerr effect in these materials. The data support the presence of two classes of particles. Generally, the nonlinearity is due to two contributions, one originating from free carriers in particles without traps, the other one originating from trapped carriers in particles with traps.

The second contribution which is often dominant for a fresh sample disappears upon darkening. The relative magnitude of the two contributions depends on the origin and on the past history of the sample and is difficult to assess a priori. The best way of determining it is to time-resolve the nonlinear response at low enough intensity. We also observed that, for the free-carrier contribution, induced absorption almost cancels absorption saturation. This indicates that, even in the strong confinement regime, quantum dots do not simply behave as two-level systems.

It is also shown that frequency-dependent measurements do not allow to determine the origin of the nonlinear response. Finally, we have reported experimental observations supporting the idea that photodarkening modifies the linear absorption spectrum through a static Kerr effect and speculated on the increase of the nonradiative decay rate in particles without traps although further experiments are needed in this last case.

References

1. Al.L. Efros, A.L. Efros: Sov. Phys.-Semicond. **16**, 772 (1982)
2. L.E. Brus: J. Chem. Phys. **80**, 4403 (1984)
3. M. Ghanassi, M.C. Schanne-Klein, F. Hache, A.I. Ekimov, D. Ricard, C. Flytzanis: Appl. Phys. Lett. **62**, 78 (1993) and references therein
4. M.G. Bawendi, W.L. Wilson, L. Rothberg, P.J. Carroll, T.M. Jedju, M.L. Steigerwald, L.E. Brus: Phys. Rev. Lett. **65**, 1623 (1990)
5. N. Peyghambarian, B. Fluegel, D. Hulin, A. Migus, M. Joffre, A. Antonetti, S.W. Koch, M. Lindberg: IEEE J. QE-**25**, 2516 (1989)
6. P. Roussignol, D. Ricard, C. Flytzanis, N. Neuroth: Phys. Rev. Lett. **62**, 312 (1989)
7. R.K. Jain, R.C. Lind: J. Opt. Soc. Am. **73**, 647 (1983)
8. A.I. Ekimov, F. Hache, M.C. Schanne-Klein, D. Ricard, C. Flytzanis, I.A. Kudryavtsev, T.V. Yazeva, A.V. Rodina, A.P.L. Efros: J. Opt. Soc. Am. B**10**, 100 (1993)
9. S. Schmitt-Rink, D.A.B. Miller, D.S. Chemla: Phys. Rev. B**35**, 8113 (1987)
10. P. Roussignol, D. Ricard, K.C. Rustagi, C. Flytzanis: Opt. Commun. **55**, 143 (1985)
11. A. Henglein, A. Kumar, E. Janata, H. Weller: Chem. Phys. Lett. **132**, 133 (1986)
12. E.F. Hilinski, P.A. Lucas, Y. Wang: J. Chem. Phys. **89**, 3435 (1988)
13. M.C. Schanne-Klein, F. Hache, D. Ricard, C. Flytzanis: J. Opt. Soc. Am. B**9**, 2234 (1992)
14. M.G. Bawendi, P.J. Carroll, W.L. Wilson, L.E. Brus: J. Chem. Phys. **96**, 946 (1992)
15. G. Bret, F. Gires: Appl. Phys. Lett **4**, 175 (1964)
16. K.W. DeLong, A. Gabel, C.T. Seaton, G.I. Stegeman: J. Opt. Soc. Am. B **6**, 1306 (1989)
17. P.N. Butcher, D. Cotter: *The Elements of Nonlinear Optics* (Cambridge Univ. Press, Cambridge 1990) p. 188
    D.L. Mills: *Nonlinear Optics* (Springer, Berlin, Heidelberg 1991)
18. L. Banyai, Y.Z. Hu, M. Lindberg, S.W. Koch: Phys. Rev. B **38**, 8142 (1988)
19. D. Ricard, M. Ghanassi, M.C. Schanne-Klein: Opt. Commun. **108**, 311 (1994)
20. M. Tomita, T. Matsumoto, M. Matsuoka: J. Opt. Soc. Am. B**6**, 165 (1989)
21. M. O'Neil, J. Marohn, G. McLendon: Chem. Phys. Lett. **168**, 208 (1991)
22. Y. Wang, A. Suna, J. McHugh, E.F. Hilinski, P.A. Lucas, R.D. Johnson: J. Chem. Phys. **92**, 6927 (1990)
23. F. Hache, D. Ricard, C. Flytzanis: Appl. Phys. Lett. **55**, 1504 (1989)
24. P. Roussignol, D. Ricard, J. Lukasik, C. Flytzanis: J. Opt. Soc. Am. B **4**, 5 (1987)
25. M. Mitsunaga, H. Shinojima, K. Kubodera: J. Opt. Soc. Am. B **5**, 1448 (1988)
26. B. van Wonterghem, S.M. Saltiel, T.E. Dutton, P.M. Rentzepis: J. Appl. Phys. **66**, 4935 (1989)
27. F. Hache, M.C. Klein, D. Ricard, C. Flytzanis: J. Opt. Soc. Am. B **8**, 1802 (1991)
28. P. Roussignol, M. Kull, D. Ricard, F. de Rougemont, R. Frey, C. Flytzanis: Appl. Phys. Lett. **51**, 1882 (1987); Erratum Appl. Phys. Lett. **54**, 1705 (1989)
29. P. Roussignol, D. Ricard, C. Flytzanis: Appl. Phys. A **44**, 285 (1987)
30. K. Kang, A.D. Kepner, Y.Z. Hu, S.W. Koch, N. Peyghambarian, C.Y. Li, T. Takada, Y. Kao, J.D. Mackenzie: Appl. Phys. Lett. **64**, 1487 (1994)
31. V.Y. Grabovskis, Y.Y. Dzenis, A.I. Ekimov, I.A. Kudryavtsev, M.N. Tolstoi, U.T. Rogulis: Sov. Phys.-Solid State **31**, 149 (1989)